

The bacterial virulence factors rhamnolipids and their (R)-3-hydroxyalkanoate precursors activate *Arabidopsis* innate immunity through two independent mechanisms

Romain Schellenberger^{a,1}, Jérôme Crouzet^{a,1}, Arvin Nickzad^b, Alexander Kutschera^c, Tim Gerster^c, Nicolas Borie^d, Corinna Dawid^e, Maude Cloutier^b, Sandra Villaume^a, Sandrine Dhondt-Cordelier^a, Jane Hubert^d, Sylvain Cordelier^a, Florence Mazeyrat-Gourbeyre^a, Christian Schmid^e, Marc Ongena^f, Jean-Hugues Renault^d, Arnaud Haudrechy^d, Thomas Hofmann^e, Fabienne Baillieul^a, Christophe Clément^a, Cyril Zipfel^{g,h}, Charles Gauthier^b, Eric Déziel^{b,2}, Stefanie Ranf^{c,2} and Stéphan Dorey^{a,2}

^a Université de Reims Champagne-Ardenne, RIBP, EA 4707, SFR Condorcet FR CNRS 3417, 51687, Reims, France

^b Centre Armand-Frappier Santé Biotechnologie, Institut national de la recherche scientifique (INRS), Laval, QC, H7V 1B7, Canada

^c Phytopathology, TUM School of Life Sciences Weihenstephan, Technical University of Munich, Freising-Weihenstephan, 85354, Germany

^d Université de Reims Champagne-Ardenne, CNRS, ICMR 7312, SFR Condorcet FR CNRS 3417, 51097, Reims France

^e Food Chemistry and Molecular Sensory Science, TUM School of Life Sciences Weihenstephan, Technical University of Munich, Freising-Weihenstephan, 85354, Germany

^f MiPI laboratory, SFR Condorcet FR CNRS 3417, Gembloux Agro-Bio Tech, University of Liège, Gembloux, B-5030, Belgium

^g The Sainsbury Laboratory, University of East Anglia, Norwich Research Park, Norwich, NR4 7UH, UK

^h Institute of Plant and Microbial Biology, Zurich-Basel Plant Science Center, University of Zurich, Zurich, Switzerland

¹ These authors contributed equally to this work.

² To whom correspondence may be addressed: E.D. (eric.deziel@inrs.ca) or S.R. (ranf@wzw.tum.de) or S.D. (stephan.dorey@univ-reims.fr).

Classification: Biological sciences; plant biology

Keywords: plant immunity, rhamnolipids, HAA, *Pseudomonas*

1 **Abstract**

2 Plant innate immunity is activated upon perception of invasion pattern molecules by plant cell-surface immune
3 receptors. Several bacteria of the genera *Pseudomonas* and *Burkholderia* produce rhamnolipids (RLs) from L-
4 rhamnose and (R)-3-hydroxyalkanoate precursors (HAAs). RL and HAA secretion is required to modulate
5 bacterial surface motility, biofilm development, and thus successful colonization of hosts. Here, we show that
6 the lipidic secretome from the opportunistic pathogen *Pseudomonas aeruginosa* mostly comprising RLs and
7 HAAs stimulates *Arabidopsis* immunity. We demonstrate that HAAs are sensed by the bulb-type lectin receptor
8 kinase LIPOOLIGOSACCHARIDE-SPECIFIC REDUCED ELICITATION/S-DOMAIN-1-29 (LORE/SD1-29) that
9 also mediates medium-chain 3-hydroxy fatty acid (mc-3-OH-FA) perception in the plant *Arabidopsis thaliana*.
10 HAA sensing induces canonical immune signaling and local resistance to plant pathogenic *Pseudomonas*
11 infection. By contrast, RLs trigger an atypical immune response and resistance to *Pseudomonas* infection
12 independent of LORE. Thus, the glycosyl moieties of RLs, albeit abolishing sensing by LORE, do not impair
13 their ability to trigger plant defense. In addition, our results show that RL-triggered immune response is affected
14 by the sphingolipid composition of the plasma membrane. In conclusion, RLs and their precursors released by
15 bacteria can both be perceived by plants but through distinct mechanisms.

16

17

18 **Significance**

19 Activation of plant innate immunity relies on the perception of microorganisms through self and nonself elicitors.
20 Rhamnolipids and their precursor HAAs are exoproducts produced by beneficial and pathogenic bacteria. They
21 are involved in bacterial surface dissemination and biofilm development. As these compounds are released in
22 the extracellular milieu, they have the potential to be perceived by the plant immune system. Our work shows
23 that both compounds independently activate plant immunity. We demonstrate that HAAs are perceived by the
24 receptor protein kinase LORE. By contrast, rhamnolipids are not sensed by LORE but activate a non-canonical
25 immune response affected by the sphingolipid composition of the plant plasma membrane. Thus, plants are
26 able to sense bacterial molecules as well as their direct precursors to trigger a distinct immune response.

27

28

29

30 Introduction

31 Plant innate immunity activation relies on detection of invasion pattern (IP) molecules that are perceived
32 by plant cells (1, 2). Non-self-recognition IPs include essential components of whole classes of microorganisms,
33 such as flagellin, peptidoglycans, mc-3-OH-FAs from bacteria or chitin and β -glucans from fungi and oomycetes,
34 respectively (3, 4). Apoplastic IPs are sensed by plant plasma membrane-localized receptor kinases (RKs) or
35 receptor-like proteins (RLPs) that function as pattern recognition receptors (PRRs) (5, 6). Activation of the
36 immune response requires the recruitment of regulatory receptor kinases and receptor-like cytoplasmic kinases
37 (RLCKs) by PRRs (7). Early cellular immune signaling of pattern-triggered immunity (PTI) includes ion-flux
38 changes at the plasma membrane, rise in cytosolic Ca^{2+} levels, production of extracellular reactive oxygen
39 species (ROS) and activation of mitogen-activated protein kinases (MAPKs) and/or Ca^{2+} -dependent protein
40 kinases (3, 8-10). Biosynthesis and mobilization of plant hormones, including salicylic acid, jasmonic acid,
41 ethylene, abscisic acid and brassinosteroids, ultimately modulate plant resistance to phytopathogens (11-14).

42 Rhamnolipids (RLs) are extracellular amphiphilic metabolites produced by several bacteria, especially
43 *Pseudomonas* and *Burkholderia* species (15-17). Acting as wetting agents, RLs are essential for the social form
44 of bacterial surface dissemination called swarming motility and for normal biofilm development (18-20). These
45 glycolipids are produced from L-rhamnose and 3-(3-hydroxyalkanoyloxy)alkanoic acid (HAA) precursors (15,
46 21). HAAs are synthesized by dimerization of (*R*)-3-hydroxyalkanoyl-CoA in *Pseudomonas*, forming congeners
47 through the RhlA enzyme (21). The opportunistic plant pathogen *Pseudomonas aeruginosa* and the
48 phytopathogen *Pseudomonas syringae* produce extracellular HAAs (16, 22-24). In *P. syringae*, HAA synthesis
49 is coordinately regulated with the late-stage flagellar gene encoding flagellin (22). HAA and RL production is
50 finely tuned and modulates the behavior of swarming migrating bacterial cells by acting as self-produced
51 negative and positive chemotactic-like stimuli (25). RLs contribute to the alteration of the bacterial outer
52 membrane composition, by shedding flagellin from the flagella (26) and by releasing lipopolysaccharides (LPS)
53 resulting in an increased hydrophobicity of the bacterial cell surface (27). In mammalian cells, RLs produced by
54 *Burkholderia plantarii* exhibit endotoxin-like properties similar to LPS, leading to the production of
55 proinflammatory cytokines in human mononuclear cells (28, 29). They also subvert the host innate immune
56 response through manipulation of the human beta-defensin-2 expression (30). Moreover, RLs from *Burkholderia*
57 *pseudomallei* induce Interferon gamma ($\text{IFN-}\gamma$)-dependent host immune response in goat (31).

58 In plants, RLs induce defense responses and resistance to biotrophic and necrotrophic pathogens (32,
59 33). They also contribute to the biocontrol activity of the plant beneficial bacterium *P. aeruginosa* PNA1 against
60 oomycetes (17). Recently, it was reported that the bulb-type lectin receptor kinase LIPOOLIGOSACCHARIDE-
61 SPECIFIC REDUCED ELICITATION/S-DOMAIN-1-29 (LORE/SD1-29) mediates medium-chain 3-hydroxy fatty
62 acid (mc-3-OH-FA) sensing in *Arabidopsis thaliana* (hereafter, *Arabidopsis*) and that bacterial compounds
63 comprising mc-3-OH-acyl building blocks including LPS and RLs do not stimulate LORE-dependent responses
64 (34).

65 Here we show that the lipidic secretome produced by *P. aeruginosa* (RLsec) mostly composed of RLs
66 and HAAs induces *Arabidopsis* immunity. HAAs are perceived through the RK LORE. We demonstrate that,
67 albeit not being sensed by LORE, RLs trigger an immune response characterized by an atypical defense
68 signature. Altogether, our results demonstrate that RLs and their precursors produced by *Pseudomonas*
69 bacteria stimulate the plant immune response by two distinct mechanisms.

70

71 Results

72 RLsec from *Pseudomonas* induces *Arabidopsis* immune responses partially mediated by LORE.

73 *Pseudomonas* species including opportunistic plant pathogenic or plant beneficial endophytic strains release a
74 mixture of RL congeners and HAA precursors, here collectively termed RL secretome (RLsec) (15, 25). HPLC-
75 MS/MS analyses of this RLsec from *P. aeruginosa* revealed the presence of mono-RLs and di-RLs at 50.9%
76 and 44.9% of dry weight, respectively, and HAAs (3.8% of dry weight) (Supplementary Table 1). RLs comprising
77 ten-carbon long lipid tails, Rha-C₁₀-C₁₀ (α -L-rhamnopyranosyl- β -hydroxydecanoyl- β -hydroxydecanoate) and
78 Rha-Rha-C₁₀-C₁₀ (α -L-rhamnopyranosyl- α -L-rhamnopyranosyl- β -hydroxydecanoyl- β -hydroxydecanoate), and
79 C₁₀-C₁₀ [(*R*)-3-(((*R*)-3-hydroxydecanoyl)oxy)decanoate] HAAs were the most abundant molecules in this lipidic
80 secretome (37.6%, 33.1%, 2.1%, respectively). Notably, low amounts of free mc-3-OH-FAs (0.4% total), such
81 as 3-OH-C₈, 3-OH-C₁₀ and 3-OH-C₁₂, were also identified (Supplementary Table 1).

82 First, we monitored apoplastic ROS production triggered by RLsec in *Arabidopsis* (35). Wild type (WT)
83 plants challenged with RLsec displayed a transient extracellular ROS production, starting at six minutes and
84 peaking at 15 minutes post elicitation (Fig. 1A). A robust ROS response was detected at concentrations of
85 RLsec starting from 0.5 μ g/mL (Fig. 1B, Supplementary Fig. 1). The ROS burst was dependent on the
86 transmembrane- NADPH oxidase RBOHD (36, 37) (Fig. 1C, Supplementary Fig. 2). RKs and RLPs mediate
87 perception of IPs and early activation of PTI signaling (7). We monitored RLsec-triggered ROS production in
88 *Arabidopsis* plants carrying loss-of-function mutations in genes encoding well characterized RKs and RLPs
89 *fls2/efr1* (38, 39), *bak1-5*, *bkk1-1*, *bak1-5/bkk1-1* (40), *bik1/pbl1* (41), *cerk1-2* (42), *sobir1-12*, *sobir1-13* (43),
90 *dorn1-1* (44) and *lore-5* (45). RLsec-induced production of ROS was only reduced in *lore-5* (Fig. 1C,
91 Supplementary Fig. 2). Some IPs, including LPS extracts and synthetic mc-3-OH-FAs, were reported to induce
92 a late ROS production in *Arabidopsis* (34, 46, 47). The late ROS response triggered by mc-3-OH-FAs was
93 dependent on LORE (34). RLsec also induced a late and long-lasting ROS burst in *Arabidopsis* culminating at
94 6-8 hours post treatment (Fig. 2A), which was abolished in *rbohD* but not in *lore-5* mutant plants (Fig. 2A).

95 Next, we tested whether RLsec induces local resistance to the hemibiotrophic phytopathogen
96 *Pseudomonas syringae* pv. *tomato* DC3000 (*Pst*) in *Arabidopsis* (48). RLsec pretreatment significantly
97 enhanced resistance against *Pst* infection in WT leaves and, although less pronounced, in *lore-5* plants (Fig.
98 2B). Taken together, our results show that RLsec induces immunity-related signaling events and disease
99 resistance in *Arabidopsis* that are partially mediated by the bulb-type lectin RK LORE.

100

101 *Pseudomonas* HAAs and mc-3-OH-FAs from RLsec trigger LORE-dependent *Arabidopsis* immunity.

102 By contrast to RLsec, purified RLs do not trigger LORE-dependent [Ca²⁺]_{cyt} and early ROS signaling
103 responses (34). Because RLsec contains significant amounts of HAAs, we investigated the role of these poorly
104 studied compounds in RLsec-triggered immunity. We compared the responses to HAA with those to mc-3-OH-
105 FAs, known to be sensed by LORE (34) and present in low amounts in RLsec (Supplementary table 1). Side-
106 by-side experiments with C₁₀-C₁₀ HAA purified from *Pseudomonas aeruginosa* secretome and 3-OH-C₁₀
107 revealed that both compounds induce [Ca²⁺]_{cyt} signaling and ROS production in WT plants in a dose-dependent
108 manner (Fig. 3A and 3B, Supplementary Fig. 3 and 4). As observed upon 3-OH-C₁₀ elicitation, purified C₁₀-C₁₀-
109 induced ROS response was impaired in *rbohD* and *lore-5* mutants (Fig. 3C). Similarly, [Ca²⁺]_{cyt} signaling

110 triggered by C₁₀-C₁₀ was impaired in *lore-5* (Fig. 3D). In addition, C₁₀-C₁₀ and 3-OH-C₁₀ both triggered LORE-
111 dependent MPK3 and MPK6 phosphorylation (Supplemental Fig. 5A). C₁₀-C₁₀ activated a late and long-lasting
112 ROS production which, unlike the RL-triggered ROS burst, was LORE-dependent (Supplemental Fig. 6). WT
113 but not *lore-5* mutant plants pretreated with C₁₀-C₁₀ or 3-OH-C₁₀ displayed enhanced resistance against *Pst*
114 (Fig. 3E). Similar to 3-OH-FAs (34), the acyl chain length of HAA affects its immune eliciting activity, as purified
115 C₁₄-C₁₄ from *B. glumae* did not induce ROS production in *Arabidopsis* plants (Supplementary Fig. 7).

116 Trace amount of 3-OH-C₁₀ was detected in C₁₀-C₁₀ purified from *P. aeruginosa* RLsec (Supplementary
117 Table 2). To avoid any influence of potential contamination of HAAs with eliciting compounds related to
118 purification procedure, we tested chemically synthesized C₁₀-C₁₀ for the ROS and [Ca²⁺]_{cyt} responses. Synthetic
119 C₁₀-C₁₀ triggered LORE-dependent [Ca²⁺]_{cyt} signaling and ROS production in a dose-dependent manner (Fig.
120 4A-C). WT plants pretreated with synthetic C₁₀-C₁₀ also displayed LORE-dependent enhanced resistance
121 against *Pst* infection (Fig. 4D).

122 Altogether, our results show that HAAs secreted by *Pseudomonas* are sensed by *Arabidopsis* through
123 the bulb-type lectin RK LORE, activate canonical PTI-related immune responses and provide resistance to
124 bacterial infection.

125

126 **RLs trigger LORE-independent *Arabidopsis* immune responses and resistance to *Pst*.**

127 To investigate whether RLs activate a LORE-independent immune response, we used purified Rha-
128 Rha-C₁₀-C₁₀ and Rha-C₁₀-C₁₀, the most abundant molecules from *P. aeruginosa* RLsec. In *Arabidopsis* WT,
129 both RL congeners induced a late and long-lasting ROS production, but as observed previously (34), no early
130 burst (Fig. 5A). As both RL congeners gave a similar ROS signature, we only used Rha-Rha-C₁₀-C₁₀ in the
131 following experiments. The minimal concentration necessary to stimulate ROS production was 50 μM with an
132 optimum at 100 μM (Fig. 5B). Late ROS production was compromised in *rbohD* but not in *lore-5* mutants (Fig.
133 5C). Surprisingly, neither MPK3 nor MPK6 activation by Rha-Rha-C₁₀-C₁₀ was detectable over a 3-hour time-
134 course (Supplementary Fig. 5B). L-Rhamnose alone was inactive demonstrating that the lipid part of the RLs is
135 necessary to trigger the immune response (Fig. 5A). *Burkholderia* species produce RL congeners with longer
136 lipid chains than those produced by *Pseudomonas* (15). The RLsec from phytopathogenic *Burkholderia glumae*
137 only contains congeners with fatty acid chain lengths varying from 12 to 16 carbons, in particular Rha-Rha-C₁₄-
138 C₁₄ (49, 50). Challenge of *Arabidopsis* with purified Rha-Rha-C₁₄-C₁₄ from *B. glumae* did not trigger any ROS
139 production (Fig. 5A) suggesting that the length of the fatty acid chain of RLs is critical for their eliciting activity.
140 To determine whether RLs trigger local resistance to pathogenic *Pseudomonas* independent of LORE, plants
141 were pretreated with 10 μM purified Rha-Rha-C₁₀-C₁₀ before *Pst* inoculation. WT plants displayed a significant
142 enhanced resistance against *Pst* that was not compromised in *lore-5* mutants (Fig. 5D).

143 To get deeper insights into the mechanisms involved in RL sensing, we used *Arabidopsis* plants carrying
144 loss-of-function mutations in genes encoding RK and RLPs but also plasma membrane channel mutants
145 including quintuple mechano-sensitive channels of small conductance-like (*msl4/5/6/9/10*) and double mid1-
146 complementing activity (*mca1/2*) channel mutants (51) that could monitor changes in membrane mechanical
147 properties. None of these mutants were affected in the long-term ROS response (Fig. 6A). Glycosylinositol
148 phosphorylceramide (GIPC) sphingolipids were recently involved in the sensing of microbial necrosis and
149 ethylene-inducing peptide 1-like (NLP) proteins (52). We found that the fatty acid hydroxylase *fah1/2* mutant

150 that is disturbed in its complex sphingolipid composition (52) showed a reduced long-term ROS response (Fig.
151 6B). Ion leakage measurement confirmed that *fah1/2* mutant plants were less affected than WT plants by RL
152 treatment (Fig. 6C). Ceramide synthase *loh1* mutants are also impaired in GIPC levels but not in glucosyl
153 ceramides (52). Interestingly, RL-triggered ROS production and ion leakage was unaltered in *loh1* plants.
154 Altogether, our results show that RLs activate an atypical immune response in *Arabidopsis* that is LORE-
155 independent, but which is affected by the sphingolipid composition of the plasma membrane.

156

157 Discussion

158 In *Pseudomonas* and *Burkholderia* species, swarming motility is intimately related to the production of
159 extracellular surface-active RLs and HAAs (22, 25, 53-55). In addition, RL production affects bacterial biofilm
160 architecture and increases affinity of cells for initial adherence to surfaces through increasing the cell's surface
161 hydrophobicity (19, 56). These exoproducts are therefore at the frontline during host colonization. Our work
162 demonstrates that both RLs and HAAs from the *Pseudomonas* lipidic secretome, referred to as RLsec here, are
163 able to trigger *Arabidopsis* innate immunity by two distinct mechanisms.

164 We found that *Pseudomonas* RLs induce an atypical immune response. This response does not involve
165 the RK LORE. Other bacterial compounds comprising mc-3-OH-acyl building blocks, but with large decorations
166 including lipid A or LPS, lipopeptides, and *N*-acyl homoserine lactones also do not trigger LORE-dependent
167 immune responses (34). RLs are glycolipids made of L-rhamnose linked to an HAA lipid tail (15, 21). Therefore,
168 glycosylation of HAAs abolishes their perception by LORE. Glycosylation is known to affect the perception of
169 IPs. Glycosylation of flg22 from *Acidovorax avenae* on Ser¹⁷⁸ and Ser¹⁸³ prevents its perception by rice cell (57).
170 Similarly, unglycosylated flagellin from *Pseudomonas syringae* pv. *tabaci* 6605 induces stronger defense
171 responses in tobacco plants than glycosylated flagellin (58). In humans, glycosylation of *Burkholderia*
172 *cenocepacia* flagellin significantly reduces its perception by epithelial cells (59).

173 We found that RL perception does not involve previously characterized RKs, RLPs or mechanosensitive
174 channels. However, the RL response is affected by alterations in sphingolipid synthesis suggesting a role of
175 these key membrane lipids in RL-triggered immunity. Recently GIPCs, major structural components of the plant
176 plasma membrane together with glucosylceramides (GlcCers), have been involved as receptors of cytotoxic
177 NLPs (52). NLPs bind terminal monomeric hexose moieties of GIPCs. Only eudicot plants are sensing these
178 NLPs through sphingolipid receptors. Insensitivity of monocots to NLPs is due to the length of the GIPC
179 headgroup, consisting of three terminal hexoses compared to two in eudicots (52). *fah1/2* mutants display
180 reduced glycosylsphingolipids (GIPCs and GlcCers) content but also lower level of ordered plasma membranes
181 (52), suggesting that, similar to the NLP response, complex sphingolipids and/or ordered plasma membranes
182 are necessary for the RL response. Unlike NLPs, RL responses were not significantly affected in *loh1* mutant
183 plants also suggesting that GlcCers more than GIPC could influence RL sensing (52). Surfactin and more
184 recently synthetic RL bolaforms and synthetic glycolipids, also active in the micromolar range, have been
185 proposed to directly interact with plasma membrane lipids (46, 60-62). Mono- and di-RLs from *Pseudomonas*
186 interact with phospholipids in several model membranes (63-66). In particular, RLs are able to fit into
187 phospholipid bilayers of plant membrane model (67). In this model, the rhamnose polar heads from RLs are
188 located near the phosphate groups from phospholipids and RL hydrophobic lipid tails are surrounded by the
189 lipid chains from these phospholipids (67). The results obtained with these plant plasma membrane models

190 suggest that the insertion of RLs into the lipid bilayer does not significantly affect lipid dynamics. The nature of
191 the phytosterols could however influence the RL effect on plant plasma membrane destabilization. Subtle
192 changes in lipid dynamics could then be linked to plant defense induction (67). Interestingly, RL bolaforms, like
193 natural RLs are inducing a non-canonical defense signature with a long-lasting oxidative burst without MPK3 or
194 MPK6 activation (46). This atypical defense signature triggered by two structurally different RLs, displaying
195 amphiphilic properties and biological activities at the micromolar range, could suggest a direct interaction of
196 these molecules with plant plasma membrane lipids.

197 We also demonstrated that HAAs, found in large amount in *Pseudomonas* lipidic secretome, are IPs
198 perceived by *Arabidopsis*. HAA sensing is mediated by LORE (34). HAAs, in the micromolar range, induce
199 typical PTI responses including transient ROS production, $[Ca^{2+}]_{cyt}$ signaling, and MPK3 and MPK6
200 phosphorylation in *Arabidopsis*. Interestingly, 3-OH-C₁₀ activates similar responses but at concentrations 10 to
201 50 times lower. This is intriguing, because HAAs are present in much larger quantities (more than 3%) compared
202 to 3-OH-FAs (0.3%) in the lipid secretome (Supplemental table 1). This high amount of HAAs could therefore
203 compensate for their lower activity. RLs are activating an immune response at relatively high concentrations
204 compared to both compounds. Interestingly, the RL concentration in the *P. aeruginosa* lipidic secretome is 10
205 to 100 times higher than HAAs and usually in the millimolar range (23, 68). RLs are produced between 20 and
206 110 μ M *in vivo* in mammals infected by *P. aeruginosa*, especially during cystic fibrosis disease (69-71). The
207 high concentrations of RLs needed for plant elicitation are in the range of the concentrations produced by the
208 bacteria.

209 Higher steric hindrance of HAA compared to 3-OH-FAs likely results in a lower affinity to the LORE
210 receptor. Synthetic ethyl 3-hydroxydecanoate (Et-3-OH-C₁₀:0) and *n*-butyl 3-hydroxydecanoate (*n*But-3-OH-
211 C₁₀:0), which possess unbranched ester-bound carbon chains in place of the carboxyl group, also triggered
212 LORE-dependent immune signaling in *Arabidopsis*, while 3-branched *tert*-butyl 3-hydroxydecanoate (*t*But-3-
213 OH-C₁₀:0) was inactive (34). HAAs, possessing a 2-branched ester-bound headgroup, activate LORE signaling.
214 The differences in efficacy could be explained by the different steric hindrance of the molecules. Alternatively,
215 the additional carboxyl group could account for the LORE-eliciting activity of HAAs.

216 *Pantoea*, *Dickeya* and *Pseudomonas* bacteria, in particular the well-known phytopathogen *P. syringae*
217 mainly produce HAAs containing 3-hydroxydecanoic acid (C₁₀) tails (15, 22, 72). By contrast, *Burkholderia*
218 species including the phytopathogenic bacterium *B. glumae*, mainly produce HAAs comprising 3-
219 hydroxytetradecanoic acid (C₁₄) tails (49). *Pseudomonas* C₁₀-containing HAAs activated *Arabidopsis* PTI
220 whereas *Burkholderia* HAAs containing C₁₄ fatty acid did not. Chain-length specificity was also observed for
221 mc-3-OH-FA sensing by the LORE receptor with 3-OH-C₁₀ representing the strongest immune elicitor (34). Thus,
222 it could be hypothesized that *Arabidopsis*, and more generally *Brassicaceae* (73), are able to specifically
223 recognize HAAs from specific bacterial species, among which several are plant opportunistic and
224 phytopathogens (74-77). Interestingly, transcript profiles of the bean pathogen *P. syringae* pv. *syringae* B728a
225 support a model in which leaf surface or epiphytic sites specifically favor swarming motility based on HAA
226 surfactant production (55, 78). Low levels of HAAs contributing to motility are produced by these bacteria (22).
227 HAA concentrations necessary to stimulate *Arabidopsis* innate immunity are in line with the concentration
228 detected in RLsec and are produced by *Pseudomonas* (between 3 to 20% of the secretome) (23, 68, 79).

229 Low amounts of free mc-3-OH-FAs were found in RLsec from *P. aeruginosa* (Supplementary table 1).
230 In *Pseudomonas*, the outer membrane lipase PagL releases 3-OH-C₁₀ during synthesis of penta-acylated lipid
231 A (34). The further fate of this 3-OH-C₁₀ is unknown. RLs are able to extract LPS from the outer membrane of
232 *P. aeruginosa* (27). Conceivably, surface-active RLs, and presumably also HAAs, could release free 3-OH-C₁₀,
233 produced through PagL activity, along with LPS from the bacterial cell wall or outer membrane vesicles (27).
234 Alternatively, degradation of HAAs/RLs *in planta* may also release free 3-OH-C₁₀. Acyl carrier protein (ACP)-
235 and coenzyme A (CoA)-bound mc-3-OH-FAs are precursors of HAA/RL synthesis (21). Upon bacterial cell lysis,
236 enzymatic or non-enzymatic degradation processes may also generate free 3-OH-C₁₀ from these precursors.
237 *In vivo*, insights into IP release have been recently obtained for flagellin. The plant glycosidase BGAL1 facilitates
238 the release of immunogenic peptides from glycosylated flagellin, upstream of cleavage by proteases (80). The
239 pathogen may evade detection by altering flagellin glycosylation and inhibiting the plant glycosidase. Flagellin
240 glycosylation increases its physical stability that could contribute to the non-liberation/recognition of the flg22
241 epitope (58, 81). RLs are able to shed flagellin from *P. aeruginosa* flagella (26), suggesting that these
242 biosurfactants participate in the release of this and presumably other eliciting compounds.

243 In conclusion, we hypothesize that when HAA- and RL-producing *Pseudomonas* colonize the leaf or
244 root surface, they release RLs and HAAs which are necessary for surface motility, biofilm development, and
245 thus successful colonization. Whereas *Arabidopsis* senses HAAs and mc-3-OH-FAs through the bulb-type lectin
246 receptor kinase LORE, RLs are perceived through a LORE-independent mechanism. In addition to direct
247 activation of a non-canonical defense response in plants, RLs, by releasing other IPs from bacteria, could
248 orchestrate a node leading to strong activation of plant immunity.

249
250

251 **Methods**

252 **Molecules.** The *P. aeruginosa* lipidic secretome used in this study was obtained from Jeneil Biosurfactant Co.,
253 Saukville, USA (JBR-599, lot. #050629). Rha-Rha-C₁₀-C₁₀ and Rha-C₁₀-C₁₀ were purified from this lipidic
254 secretome mixture, as previously described (33, 34). Rha-Rha-C₁₄-C₁₄ were purified from the *B. glumae* lipidic
255 secretome (49). To obtain pure HAAs from *P. aeruginosa* or *B. glumae*, RLs were hydrolyzed using 1 M HCl in
256 1:1 dioxane-water boiling at reflux for 60 min. The mixture was extracted with ethyl acetate and the extracts
257 were dried over anhydrous Na₂SO₄. After filtration, the resulting extracts were then evaporated to dryness and
258 resuspended in 2 mL of methanol. HAAs were then isolated from digested mixture using flash chromatography
259 on a Biotage (Stockholm, Sweden) Isorela One instrument with a SNAP Ultra C18 12g column (Biotage) using
260 an acetonitrile/water gradient at 12 mL/min flow rate. The elution was started with 0% acetonitrile for 4.5 min
261 and the acetonitrile concentration was raised to 100% over 28.2 min, followed by an isocratic elution of 100%
262 acetonitrile for 13.3 min. The flash chromatography fraction containing the C₁₀-C₁₀ was further separated and
263 purified using 0.25 mm thin-layer chromatographic (TLC) plates (SiliCycle SilicaPlate F-254) and developed
264 with *n*-hexane-ethyl acetate-acetic acid (24:74:2). The bands were scraped from the plates and the HAAs,
265 including C₁₀-C₁₀, were extracted from the silica with chloroform-methanol (5:1). 3-OH-C₁₀ was purchased from
266 Sigma-Aldrich Saint-Quentin Fallavier, France. All compounds were dissolved in ethanol or methanol as
267 indicated to prepare stock solutions. Final aqueous compound dilutions were prepared freshly on the days of
268 the experiment. Control solutions contained equal amounts of ethanol or methanol (0.05% for most experiments

269 and not exceeding 0.5% for the highest concentrations tested). Chemical synthesis of C₁₀-C₁₀ is described in
270 supplementary data 1 and 2.

271

272 **LC-MS analysis of HAAs.** Samples were prepared by diluting stock solutions using MeOH to final concentration
273 of 50 ppm. 16-Hydroxyhexadecanoic acid at 20 ppm was added to samples as internal standard⁷¹. The analyses
274 were performed with a Quattro II triple quadrupole mass spectrometer (Micromass, Pointe-Claire, Canada)
275 equipped with a Z-spray interface using electrospray ionization in negative mode. The capillary voltage was set
276 at 3.5 kV and the cone voltage at 25 V. The source temperature was kept at 120°C and the desolvation gas at
277 150°C. The scanning mass range was from 130 to 930 Da. The instrument was interfaced to a high-performance
278 liquid chromatograph (HPLC; Waters 2795, Mississauga, Ontario, Canada) equipped with a 100 x 4 mm i.d.
279 Luna Omega PS C18 reversed-phase column (particle size 5 µm) using a water-acetonitrile gradient with a
280 constant 2 mmol L⁻¹ concentration of ammonium acetate (0.6 mL.min⁻¹). Quantification of free 3-OH-C₁₀ in
281 purified C₁₀-C₁₀, Rha-Rha-C₁₀-C₁₀, Rha-C₁₀-C₁₀, Rha-Rha-C₁₄-C₁₄ or synthetic C₁₀-C₁₀ were performed as
282 reported previously (34) and are presented in Supplementary table 2.

283

284 **Plant material and growth conditions.** *Arabidopsis thaliana* ecotype Col-0 was used as WT parent for all
285 experiments. Seeds from *fls2/efr1* (38, 39), *bak1-5*, *bkk1-1*, *bak1-5/bkk1-1* (40), *cerk1-2* (42), *bik1/pbl1* (41),
286 *rbohD*, *msl4/5/6/9/10* and *mca1/2* (51) were provided by C. Zipfel. Seeds from *sobir1-12* and *sobir1-13* (43)
287 were provided by F. Brunner (Center for Plant Molecular Biology, University of Tübingen, Tübingen,
288 PlantResponse™). Seeds from *sd1-29* (*lore-5*), Col-0^{AEQ} and *lore-5*^{AEQ} were provided by S. Ranf (45). *loh1* and
289 *fah1/2* seed (52) were provided by I. Feussner (University of Göttingen, Germany). *dorn1-1* seeds (44) were
290 obtained from NASC stock (SALK_042209). All mutants are in the Col-0 background. Plants were grown on soil
291 in growth chambers at 20°C, under 12 h light / 12 h dark regime with fluorescent light of 150 µmol m⁻² s⁻¹ and
292 60% relative humidity.

293

294 **Extracellular ROS production and calcium signaling.** ROS assays were performed on 4- to 6-week-old
295 *Arabidopsis* plants cultured on soil. Briefly, 5 mm long petiole sections were cut and placed in 150 µL of distilled
296 water overnight in 96 wells plate (PerkinElmer) (46). Then, the protocol was conducted as previously described
297 (82). Luminescence (relative light units, RLU) was measured every 2 min during 46 or 720 min with a Tecan
298 Infinite F200 PRO (or a TECAN CM SPARK for Supplementary figure 6), Tecan France. Total ROS production
299 was calculated by summing RLU measured between 4 to 46 or 4 to 720 minutes after treatment. Control was
300 realized on petioles of WT or mutant plants. [Ca²⁺]_{cyt} measurements were done as previously described (34).

301

302 **MAPK phosphorylation assays.** For MAPK phosphorylation assays, 3 leaf disks (9 mm diameter) were
303 collected from 4 to 6-week-old *Arabidopsis* plants grown on soil and incubated 8 h in distilled water. Leaf disks
304 were mock-treated or treated with different molecules. 15 min, 1 hour, and 3 hours after treatment, plant tissues
305 were frozen in liquid nitrogen. To extract proteins, 60 mg of leaf tissues were ground in a homogenizer Potter-
306 Elvehjem with 60 µL of extraction buffer (0.35 M Tris-HCl (pH 6.8), 30% (v/v) glycerol, 10% (v/v) SDS, 0.6 M
307 DTT, 0.012% (w/v) bromophenol blue). Total protein extracts were denatured for 7 min at 95°C, centrifuged at
308 11 000g for 5 min and 30 µL of supernatant were separated by 12% SDS-PAGE. Proteins were transferred onto

309 PVDF membranes for 10 min at 25 V using iBLOT gel transfer system (Invitrogen). After 30 min in 5% saturation
310 solution (50 g L⁻¹ milk, TBS (137 mM NaCl, 2.7 mM KCl, 25 mM Tris-HCl), Tween20 0.05% (v/v)) and 3 times 5
311 min in 0.5% washing solution (5 g L⁻¹ milk, TBS (137 mM NaCl, 2.7 mM KCl, 25 mM Tris-HCl), Tween 20 0.05%
312 (v/v)), membranes were incubated overnight with rabbit polyclonal primary antibodies against phospho-p44/42
313 MAPK (Erk1/2) (Cell Signaling, 1:2000) at 4°C. Then, membranes were washed 3 times 5 min with washing
314 solution and incubated 1 h with anti-rabbit IgG HRP-conjugated secondary antibodies (Bio-Rad, 1:3000) at room
315 temperature. Finally, washed membranes were developed with SuperSignal® West Femto using an odyssey
316 scanner (ODYSSEY® Fc Dual-Mode Imaging System, LI-COR). To normalize protein loading, membranes were
317 stripped 15 min with 0.25 M NaOH, blocked 30 min in 5% non-fat milk. Then, membranes were incubated at
318 room temperature for 1 h with plant monoclonal anti-actin primary antibodies (CusAb, 1:1000) and 1 h with anti-
319 mouse IgG HRP-conjugated secondary antibodies (Cell Signaling, 1:3000). Membranes were washed and
320 developed as described above.

321
322 **Conductivity assay.** The assay was performed as described previously (83), with few modifications. Eight leaf
323 discs of 6-mm-diameter were incubated in distilled water overnight. One disc was transferred into 1.5 mL tube
324 containing fresh distilled water and the corresponding elicitor concentration or ethanol for control. Conductivity
325 measurements (three to four replicates for each treatment) were then conducted using a B-771 LaquaTwin
326 (Horiba) conductivity meter.

327
328 ***Pseudomonas syringae* culture and disease resistance assays.** *Pseudomonas syringae* pv. *tomato* strain
329 DC3000 was grown at 28°C under stirring in King's B (KB) liquid medium supplemented with antibiotics: 50 µg
330 mL⁻¹ of rifampicin and 50 µg mL⁻¹ of kanamycin. For local protection assays, 15 seeds were sown per pot and
331 grown for 3 to 5 weeks in soil. Plants were sprayed with molecules or ethanol as control and were placed two
332 days in high humidity atmosphere before infections. Plants were inoculated by spraying the leaves with 3 mL of
333 a bacterial suspension at an optical density (OD₆₀₀) of 0.01 (0.025 % Silwet L-77, 10 mM MgCl₂). Quantification
334 (colony forming units) of *in planta* bacterial growth was performed 3 dpi. To this end, all plant leaves from the
335 same pot were harvested, weighed, and crushed in a mortar with 10 mL of 10 mM MgCl₂ and serial dilutions
336 were performed. For each dilution, 10 µL were dropped on KB plate supplemented with appropriate antibiotics.
337 Colony forming units (CFU) were counted after 2 days of incubation at 28°C. The number of bacteria per mg of
338 plants fresh mass was obtained with the formula:

339

$$340 \quad \text{CFU.mg}^{-1} = \frac{\left(\frac{N \times V_d}{V_i} \times 10^{(n-1)} \times 100 \right)}{M}$$

341
342 with N equal to CFU number, V_i the volume depot on plate, V_d the total volume, n the dilution number and M
343 the plants fresh mass.

344
345 **References**

- 346 1. D. E. Cook, C. H. Mesarich, B. P. Thomma, Understanding plant immunity as a surveillance system to
347 detect invasion. *Annu. Rev. Phytopathol.* **53**, 541-563 (2015).

- 348 2. K. Kanyuka, J. J. Rudd, Cell surface immune receptors: the guardians of the plant's extracellular spaces.
349 *Curr. Opin. Plant Biol.* **50**, 1-8 (2019).
- 350 3. T. Boller, G. Felix, A renaissance of elicitors: perception of microbe-associated molecular patterns and
351 danger signals by pattern-recognition receptors. *Annu. Rev. Plant Biol.* **60**, 379-406 (2009).
- 352 4. M. A. Newman, T. Sundelin, J. T. Nielsen, G. Erbs, MAMP (microbe-associated molecular pattern)
353 triggered immunity in plants. *Front. Plant Sci.* **4**, 139 (2013).
- 354 5. F. Boutrot, C. Zipfel, Function, discovery, and exploitation of plant pattern recognition receptors for
355 broad-spectrum disease resistance. *Annu. Rev. Phytopathol.* **55**, 257-286 (2017).
- 356 6. S. Ranf, Sensing of molecular patterns through cell surface immune receptors. *Curr. Opin. Plant Biol.*
357 **38**, 68-77 (2017).
- 358 7. D. Couto, C. Zipfel, Regulation of pattern recognition receptor signalling in plants. *Nat. Rev. Immunol.*
359 **16**, 537-552 (2016).
- 360 8. J. Bigeard, J. Colcombet, H. Hirt, Signaling mechanisms in pattern-triggered immunity (PTI). *Mol. Plant*
361 **8**, 521-539 (2015).
- 362 9. A. Garcia-Brugger *et al.*, Early signaling events induced by elicitors of plant defenses. *Mol. Plant-
363 Microbe Interact.* **19**, 711-724 (2006).
- 364 10. S. Wu, L. Shan, P. He, Microbial signature-triggered plant defense responses and early signaling
365 mechanisms. *Plant Sci.* **228**, 118-126 (2014).
- 366 11. D. De Vleeschauwer, G. Gheysen, M. Hofte, Hormone defense networking in rice: tales from a different
367 world. *Trends Plant Sci.* **18**, 555-565 (2013).
- 368 12. J. Glazebrook, Contrasting mechanisms of defense against biotrophic and necrotrophic pathogens.
369 *Annu. Rev. Phytopathol.* **43**, 205-227 (2005).
- 370 13. A. Robert-Seilaniantz, M. Grant, J. D. Jones, Hormone crosstalk in plant disease and defense: more
371 than just jasmonate-salicylate antagonism. *Annu. Rev. Phytopathol.* **49**, 317-343 (2011).
- 372 14. L. Trda *et al.*, Perception of pathogenic or beneficial bacteria and their evasion of host immunity: pattern
373 recognition receptors in the frontline. *Front. Plant Sci.* **6**, 219 (2015).
- 374 15. A. M. Abdel-Mawgoud, F. Lépine, E. Déziel, Rhamnolipids: diversity of structures, microbial origins and
375 roles. *Appl. Microbiol. Biotechnol.* **86**, 1323-1336 (2010).
- 376 16. V. U. Irorere, L. Tripathi, R. Marchant, S. McClean, I. M. Banat, Microbial rhamnolipid production: a
377 critical re-evaluation of published data and suggested future publication criteria. *Appl. Microbiol.
378 Biotechnol.* **101**, 3941-3951 (2017).
- 379 17. M. Perneel *et al.*, Phenazines and biosurfactants interact in the biological control of soil-borne diseases
380 caused by *Pythium* spp. *Environ. Microbiol.* **10**, 778-788 (2008).
- 381 18. L. Chrzanowski, L. Lawniczak, K. Czaczyk, Why do microorganisms produce rhamnolipids? *World J.
382 Microbiol. Biotechnol.* **28**, 401-419 (2012).
- 383 19. A. Nickzad, E. Déziel, The involvement of rhamnolipids in microbial cell adhesion and biofilm
384 development - an approach for control? *Lett. Appl. Microbiol.* **58**, 447-453 (2014).
- 385 20. P. Vatsa, L. Sanchez, C. Clément, F. Baillieul, S. Dorey, Rhamnolipid biosurfactants as new players in
386 animal and plant defense against microbes. *Int. J. Mol. Sci.* **11**, 5095-5108 (2010).
- 387 21. A. M. Abdel-Mawgoud, F. Lépine, E. Déziel, A stereospecific pathway diverts beta-oxidation
388 intermediates to the biosynthesis of rhamnolipid biosurfactants. *Chem. Biol.* **21**, 156-164 (2014).
- 389 22. A. Y. Burch *et al.*, *Pseudomonas syringae* coordinates production of a motility-enabling surfactant with
390 flagellar assembly. *J. Bacteriol.* **194**, 1287-1298 (2012).
- 391 23. E. Déziel, F. Lépine, S. Milot, R. Villemur, *rhlA* is required for the production of a novel biosurfactant
392 promoting swarming motility in *Pseudomonas aeruginosa*: 3-(3-hydroxyalkanoyloxy)alkanoic acids
393 (HAAs), the precursors of rhamnolipids. *Microbiology* **149**, 2005-2013 (2003).
- 394 24. J. M. Plotnikova, L. G. Rahme, F. M. Ausubel, Pathogenesis of the human opportunistic pathogen
395 *Pseudomonas aeruginosa* PA14 in *Arabidopsis*. *Plant Physiol.* **124**, 1766-1774 (2000).

- 396 25. J. Tremblay, A. P. Richardson, F. Lépine, E. Déziel, Self-produced extracellular stimuli modulate the
397 *Pseudomonas aeruginosa* swarming motility behaviour. *Environ. Microbiol.* **9**, 2622-2630 (2007).
- 398 26. U. Gerstel, M. Czapp, J. Bartels, J. M. Schroder, Rhamnolipid-induced shedding of flagellin from
399 *Pseudomonas aeruginosa* provokes hBD-2 and IL-8 response in human keratinocytes. *Cell. Microbiol.*
400 **11**, 842–853 (2009).
- 401 27. R. A. Al-Tahhan, T. R. Sandrin, A. A. Bodour, R. M. Maier, Rhamnolipid-induced removal of
402 lipopolysaccharide from *Pseudomonas aeruginosa*: effect on cell surface properties and interaction with
403 hydrophobic substrates. *Appl. Environ. Microbiol.* **66**, 3262-3268 (2000).
- 404 28. J. Andrä *et al.*, Endotoxin-like properties of a rhamnolipid exotoxin from *Burkholderia (Pseudomonas)*
405 *plantarii*: immune cell stimulation and biophysical characterization. *Biol. Chem.* **387**, 301-310 (2006).
- 406 29. J. Bauer, K. Brandenburg, U. Zahringer, J. Rademann, Chemical synthesis of a glycolipid library by a
407 solid-phase strategy allows elucidation of the structural specificity of immunostimulation by rhamnolipids.
408 *Chemistry* **12**, 7116-7124 (2006).
- 409 30. J. Dossel, U. Meyer-Hoffert, J. M. Schroder, U. Gerstel, *Pseudomonas aeruginosa*-derived
410 rhamnolipids subvert the host innate immune response through manipulation of the human beta-
411 defensin-2 expression. *Cell. Microbiol.* **14**, 1364-1375 (2012).
- 412 31. M. Gonzalez-Juarrero *et al.*, Polar lipids of *Burkholderia pseudomallei* induce different host immune
413 responses. *PloS one* **8**, e80368 (2013).
- 414 32. L. Sanchez *et al.*, Rhamnolipids elicit defense responses and induce disease resistance against
415 biotrophic, hemibiotrophic, and necrotrophic pathogens that require different signaling pathways in
416 *Arabidopsis* and highlight a central role for salicylic acid. *Plant Physiol.* **160**, 1630-1641 (2012).
- 417 33. A. L. Varnier *et al.*, Bacterial rhamnolipids are novel MAMPs conferring resistance to *Botrytis cinerea* in
418 grapevine. *Plant, Cell Environ.* **32**, 178-193 (2009).
- 419 34. A. Kutschera *et al.*, Bacterial medium-chain 3-hydroxy fatty acid metabolites trigger immunity in
420 *Arabidopsis* plants. *Science* **364**, 178-181 (2019).
- 421 35. J. Qi, J. Wang, Z. Gong, J. M. Zhou, Apoplastic ROS signaling in plant immunity. *Curr. Opin. Plant Biol.*
422 **38**, 92-100 (2017).
- 423 36. Y. Kadota, K. Shirasu, C. Zipfel, Regulation of the NADPH oxidase RBOHD during plant immunity. *Plant*
424 *Cell Physiol.* **56**, 1472-1480 (2015).
- 425 37. M. A. Torres, J. L. Dangl, J. D. Jones, *Arabidopsis* gp91phox homologues AtrbohD and AtrbohF are
426 required for accumulation of reactive oxygen intermediates in the plant defense response. *Proc. Natl.*
427 *Acad. Sci. USA* **99**, 517-522 (2002).
- 428 38. D. Chinchilla, Z. Bauer, M. Regenass, T. Boller, G. Felix, The *Arabidopsis* receptor kinase FLS2 binds
429 flg22 and determines the specificity of flagellin perception. *Plant Cell* **18**, 465-476 (2006).
- 430 39. C. Zipfel *et al.*, Perception of the bacterial PAMP EF-Tu by the receptor EFR restricts *Agrobacterium*-
431 mediated transformation. *Cell* **125**, 749-760 (2006).
- 432 40. M. Roux *et al.*, The *Arabidopsis* leucine-rich repeat receptor-like kinases BAK1/SERK3 and
433 BKK1/SERK4 are required for innate immunity to hemibiotrophic and biotrophic pathogens. *Plant Cell*
434 **23**, 2440-2455 (2011).
- 435 41. L. Li *et al.*, The FLS2-associated kinase BIK1 directly phosphorylates the NADPH oxidase RbohD to
436 control plant immunity. *Cell Host Microbe* **15**, 329-338 (2014).
- 437 42. A. Miya *et al.*, CERK1, a LysM receptor kinase, is essential for chitin elicitor signaling in *Arabidopsis*.
438 *Proc. Natl. Acad. Sci. USA* **104**, 19613-19618 (2007).
- 439 43. W. Zhang *et al.*, *Arabidopsis* receptor-like protein30 and receptor-like kinase suppressor of BIR1-
440 1/EVERSHED mediate innate immunity to necrotrophic fungi. *Plant Cell* **25**, 4227-4241 (2013).
- 441 44. J. Choi *et al.*, Identification of a plant receptor for extracellular ATP. *Science* **343**, 290-294 (2014).
- 442 45. S. Ranf *et al.*, A lectin S-domain receptor kinase mediates lipopolysaccharide sensing in *Arabidopsis*
443 *thaliana*. *Nat. Immunol.* **16**, 426-433 (2015).

- 444 46. P. Luzuriaga-Loaiza *et al.*, Synthetic rhamnolipid bolaforms trigger an innate immune response in
445 *Arabidopsis thaliana*. *Sci. Rep.* **8**, 8534 (2018).
- 446 47. K. Shang-Guan *et al.*, Lipopolysaccharides trigger two successive bursts of reactive oxygen species at
447 distinct cellular locations. *Plant Physiol.* **176**, 2543-2556 (2018).
- 448 48. X. F. Xin, S. Y. He, *Pseudomonas syringae* pv. *tomato* DC3000: a model pathogen for probing disease
449 susceptibility and hormone signaling in plants. *Annu. Rev. Phytopathol.* **51**, 473-498 (2013).
- 450 49. S. G. Costa, E. Déziel, F. Lépine, Characterization of rhamnolipid production by *Burkholderia glumae*.
451 *Lett. Appl. Microbiol.* **53**, 620-627 (2011).
- 452 50. J. H. Ham, R. A. Melanson, M. C. Rush, *Burkholderia glumae*: next major pathogen of rice? *Mol. Plant*
453 *Pathol.* **12**, 329-339 (2011).
- 454 51. A. B. Stephan, H. H. Kunz, E. Yang, J. I. Schroeder, Rapid hyperosmotic-induced Ca²⁺ responses in
455 *Arabidopsis thaliana* exhibit sensory potentiation and involvement of plastidial KEA transporters. *Proc.*
456 *Natl. Acad. Sci. USA* **113**, E5242-5249 (2016).
- 457 52. T. Lenarcic *et al.*, Eudicot plant-specific sphingolipids determine host selectivity of microbial NLP
458 cytolysins. *Science* **358**, 1431-1434 (2017).
- 459 53. N. C. Caiazza, R. M. Shanks, G. A. O'Toole, Rhamnolipids modulate swarming motility patterns of
460 *Pseudomonas aeruginosa*. *J. Bacteriol.* **187**, 7351-7361 (2005).
- 461 54. A. Nickzad, F. Lépine, E. Déziel, Quorum sensing controls swarming motility of *Burkholderia glumae*
462 through regulation of rhamnolipids. *PloS one* **10**, e0128509 (2015).
- 463 55. X. Yu *et al.*, Transcriptional responses of *Pseudomonas syringae* to growth in epiphytic versus
464 apoplastic leaf sites. *Proc. Natl. Acad. Sci. USA* **110**, E425-434 (2013).
- 465 56. M. E. Davey, N. C. Caiazza, G. A. O'Toole, Rhamnolipid surfactant production affects biofilm
466 architecture in *Pseudomonas aeruginosa* PAO1. *J. Bacteriol.* **185**, 1027-1036 (2003).
- 467 57. H. Hirai *et al.*, Glycosylation regulates specific induction of rice immune responses by *Acidovorax*
468 *avenae* flagellin. *J. Biol. Chem.* **286**, 25519-25530 (2011).
- 469 58. F. Taguchi *et al.*, Glycosylation of flagellin from *Pseudomonas syringae* pv. *tabaci* 6605 contributes to
470 evasion of host tobacco plant surveillance system. *Physiol. Mol. Plant Pathol.* **74**, 11-17 (2009).
- 471 59. A. Hanuszkiewicz *et al.*, Identification of the flagellin glycosylation system in *Burkholderia cenocepacia*
472 and the contribution of glycosylated flagellin to evasion of human innate immune responses. *J. Biol.*
473 *Chem.* **289**, 19231-19244 (2014).
- 474 60. G. Henry, M. Deleu, E. Jourdan, P. Thonart, M. Ongena, The bacterial lipopeptide surfactin targets the
475 lipid fraction of the plant plasma membrane to trigger immune-related defence responses. *Cell.*
476 *Microbiol.* **13**, 1824-1837 (2011).
- 477 61. M. N. Nasir *et al.*, Differential interaction of synthetic glycolipids with biomimetic plasma membrane
478 lipids correlates with the plant biological response. *Langmuir* **33**, 9979-9987 (2017).
- 479 62. M. Robineau *et al.*, Synthetic mono-rhamnolipids display direct antifungal effects and trigger an innate
480 immune response in tomato against *Botrytis cinerea*. *Molecules* **25**, 3108 (2020).
- 481 63. H. Abbasi, K. A. Noghbi, A. Ortiz, Interaction of a bacterial monorhamnolipid secreted by
482 *Pseudomonas aeruginosa* MA01 with phosphatidylcholine model membranes. *Chem. Phys. Lipids* **165**,
483 745-752 (2012).
- 484 64. F. J. Aranda *et al.*, Thermodynamics of the interaction of a dirhamnolipid biosurfactant secreted by
485 *Pseudomonas aeruginosa* with phospholipid membranes. *Langmuir* **23**, 2700-2705 (2007).
- 486 65. A. Ortiz, F. J. Aranda, J. A. Teruel, Interaction of dirhamnolipid biosurfactants with phospholipid
487 membranes: a molecular level study. *Adv. Exp. Med. Biol.* **672**, 42-53 (2010).
- 488 66. M. Sanchez, F. J. Aranda, J. A. Teruel, A. Ortiz, Interaction of a bacterial dirhamnolipid with
489 phosphatidylcholine membranes: a biophysical study. *Chem. Phys. Lipids* **161**, 51-55 (2009).
- 490 67. N. Monnier *et al.*, Exploring the dual interaction of natural rhamnolipids with plant and fungal biomimetic
491 plasma membranes through biophysical studies. *Int. J. Mol. Sci.* **20**, 1009 (2019).

- 492 68. F. Lépine, E. Déziel, S. Milot, R. Villemur, Liquid chromatographic/mass spectrometric detection of the
493 3-(3-hydroxyalkanoyloxy) alkanolic acid precursors of rhamnolipids in *Pseudomonas aeruginosa*
494 cultures. *J. Mass Spectrom.* **37**, 41-46 (2002).
- 495 69. R. Kownatzki, B. Tummler, G. Doring, Rhamnolipid of *Pseudomonas aeruginosa* in sputum of cystic
496 fibrosis patients. *Lancet* **1**, 1026-1027 (1987).
- 497 70. R. C. Read *et al.*, Effect of *Pseudomonas aeruginosa* rhamnolipids on mucociliary transport and ciliary
498 beating. *J. Appl. Physiol.* **72**, 2271-2277 (1992).
- 499 71. M. Somerville *et al.*, Release of mucus glycoconjugates by *Pseudomonas aeruginosa* rhamnolipid into
500 feline trachea *in vivo* and human bronchus *in vitro*. *Am. J. Respir. Cell Mol. Biol.* **6**, 116-122 (1992).
- 501 72. A. Germer *et al.*, Exploiting the natural diversity of RhIA acyltransferases for the synthesis of the
502 rhamnolipid precursor 3-(3-Hydroxyalkanoyloxy)alkanoic acid. *Appl. Environ. Microbiol.* **86**, e02317-
503 02319 (2020).
- 504 73. S. Ranf, Immune sensing of lipopolysaccharide in plants and animals: same but different. *PLOS Pathog.*
505 **12**, e1005596 (2016).
- 506 74. S. Compant, J. Nowak, T. Coenye, C. Clément, E. Ait Barka, Diversity and occurrence of *Burkholderia*
507 spp. in the natural environment. *FEMS Microbiol. Rev.* **32**, 607-626 (2008).
- 508 75. E. Kay, F. Bertolla, T. M. Vogel, P. Simonet, Opportunistic colonization of *Ralstonia solanacearum*-
509 infected plants by *Acinetobacter* sp. and its natural competence development. *Microb. Ecol.* **43**, 291-
510 297 (2002).
- 511 76. M. W. Silby, C. Winstanley, S. A. Godfrey, S. B. Levy, R. W. Jackson, *Pseudomonas* genomes: diverse
512 and adaptable. *FEMS Microbiol. Rev.* **35**, 652-680 (2011).
- 513 77. I. K. Toth, L. Pritchard, P. R. J. Birch, Comparative genomics reveals what makes an enterobacterial
514 plant pathogen. *Annu. Rev. Phytopathol.* **44**, 305-336 (2006).
- 515 78. X. Yu *et al.*, Transcriptional analysis of the global regulatory networks active in *Pseudomonas syringae*
516 during leaf colonization. *mBio* **5**, e01683-01614 (2014).
- 517 79. K. Zhu, C. O. Rock, RhIA converts beta-hydroxyacyl-acyl carrier protein intermediates in fatty acid
518 synthesis to the beta-hydroxydecanoyl-beta-hydroxydecanoate component of rhamnolipids in
519 *Pseudomonas aeruginosa*. *J. Bacteriol.* **190**, 3147-3154 (2008).
- 520 80. P. Buscaill *et al.*, Glycosidase and glycan polymorphism control hydrolytic release of immunogenic
521 flagellin peptides. *Science* **364**, eaav0748 (2019).
- 522 81. F. Taguchi *et al.*, Effects of glycosylation on swimming ability and flagellar polymorphic transformation
523 in *Pseudomonas syringae* pv. *tabaci* 6605. *J. Bacteriol.* **190**, 764-768 (2008).
- 524 82. J. M. Smith, A. Heese, Rapid bioassay to measure early reactive oxygen species production in
525 *Arabidopsis* leave tissue in response to living *Pseudomonas syringae*. *Plant Methods* **10**, 6 (2014).
- 526 83. M. Magnin-Robert *et al.*, Modifications of sphingolipid content affect tolerance to hemibiotrophic and
527 necrotrophic pathogens by modulating plant defense responses in *Arabidopsis*. *Plant Physiol.* **169**,
528 2255-2274 (2015).
- 529 84. M. De Vleeschouwer *et al.*, Rapid total synthesis of cyclic lipodepsipeptides as a premise to investigate
530 their self-assembly and biological activity. *Chem. Eur. J.* **20**, 7766-7775 (2014).

531
532

Acknowledgments

533 We are thankful to Laetitia Parent and Sylvain Milot for technical support and Ralph Hüchelhoven for
534 critical discussion. This work was supported by grants from EliDeRham and Rhamnoprot (Région Grand Est).
535 The project Rhamnoprot is co-funded by the European Union FEDER program. Work on rhamnolipids in the
536 Déziel Lab is funded by the Natural Sciences and Engineering Research Council of Canada (NSERC) through
537 Discovery grants RGPIN-2015-03931 and RGPIN-2020-06771. Work in the Ranf lab is supported by the
538 German Research Foundation (SFB924/TP-B10 and Emmy Noether programme RA2541/1).

539

540 **Author contributions**

541 J.C. and S.D. designed the research; R.S., J.C., A.K., T.G., M.T., S.V., S.D.C. performed the
542 experiments; A.N. and E.D. purified and characterized HAAs and *B. glumae* RLs; M.C. and C.G. chemically
543 synthesized HAAs; N.B., J.H., A.H. and J.H.R., purified *P. aeruginosa* RLs; C.D. and C.S. quantified mc-3-OH-
544 FAs in all samples; R.S., J.C., S.C., F.M.G., F.B., S.R., E.D. and S.D. analyzed the data; R.S., J.C. and S.D.
545 wrote the manuscript. M.O., J.H.R., A.H., T.H., C.Z., F.B., C.C., S.R and E.D contributed ideas, and critically
546 revised the manuscript. All authors discussed the results and approved the manuscript.

547

548 **Additional Information**

549

550 **Data availability**

551 The authors declare that all data supporting the findings of this study can be found within the manuscript
552 and its Supplementary Files. Additional data supporting the findings of this study are available from the
553 corresponding authors upon request.

554

555 **Competing financial interests**

556 Technical University of Munich has filed a patent application to inventors A.K., C.D., T.H., and S.R. The
557 authors declare no financial conflicts of interest in relation to this work.

558 All other author(s) declare no competing financial and/or non-financial interests.

559

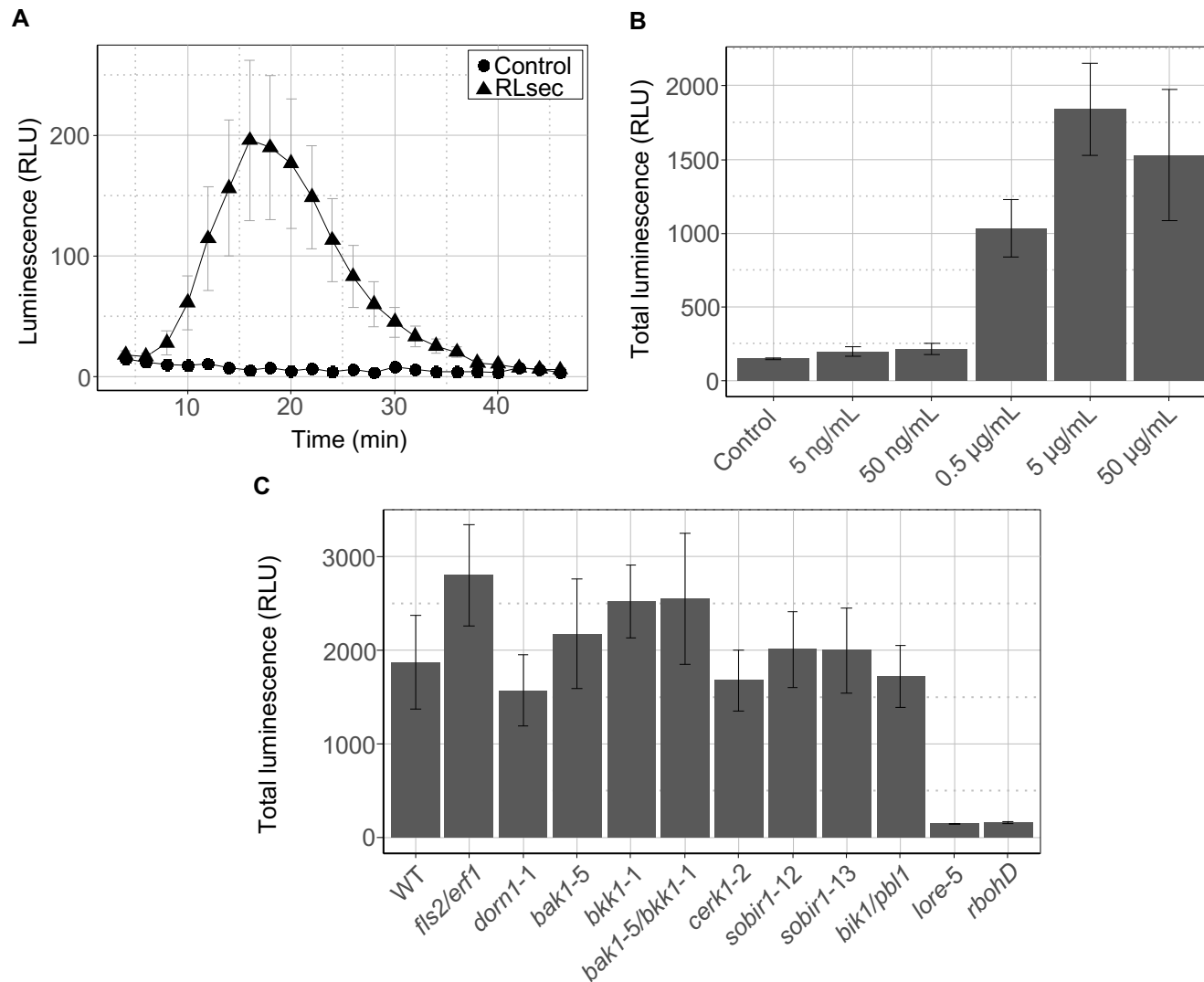


Fig. 1. RLsec activates LORE-dependent early immune-related responses in *Arabidopsis*. (A) Extracellular ROS production after treatment of WT leaf petioles with 50 µg/mL RLsec or EtOH as control. (B) Dose effect of RLsec on ROS production. ROS production measured after treatment of WT leaf petioles with the indicated concentrations of RLsec or EtOH as control. (C) ROS production measured after treatment of WT, *fls2/err1*, *dorn1-1*, *bak1-5*, *bkk1-1*, *bak1-5/bkk1-1*, *cerk1-2*, *sobir1-12*, *sobir1-13*, *bik1/pbl1*, *lore-5*, or *rbohD* leaf petioles with 50 µg/mL RLsec. (a,b,c) Data are mean ± SEM (n = 6). Experiments have been realized three times with similar results.

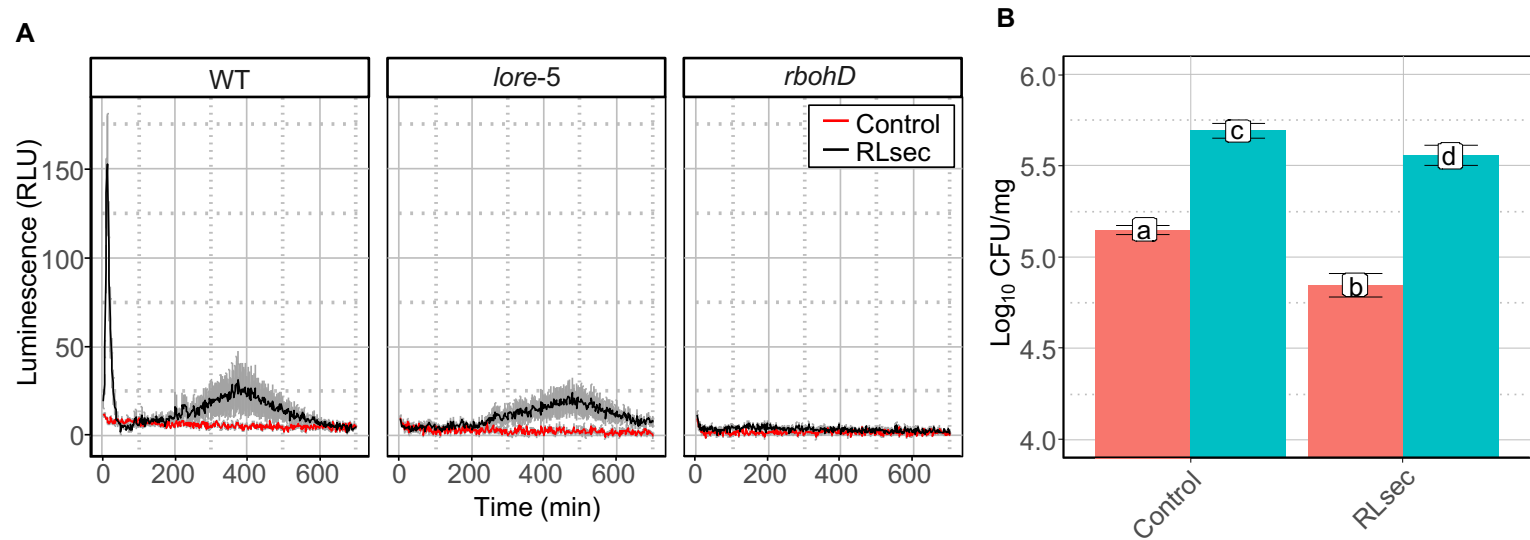


Fig. 2. RLsec activates LORE-independent responses in *Arabidopsis*. (A) Extracellular ROS production after treatment of WT, *lore-5*, and *rbohD* leaf petioles with 50 $\mu\text{g}/\text{mL}$ RLsec or EtOH (Control). ROS production was monitored over 720 minutes. Data are mean \pm SEM ($n = 6$). Experiments have been realized three times with similar results. (B) WT (red) and *lore-5* (blue) *Arabidopsis* leaves were treated with 50 $\mu\text{g}/\text{mL}$ RLsec or EtOH (control) 48 h before infection. *Pst* titers were measured at 3 d.p.i. Data are mean \pm SD ($n = 6, 5, 6, 6$ (left to right)). Experiments have been realized twice with similar results. Letters represent results of pairwise Wilcoxon-Mann-Whitney statistic test with $P > 0.05$ (same letters) or $P \leq 0.05$ (different letters).

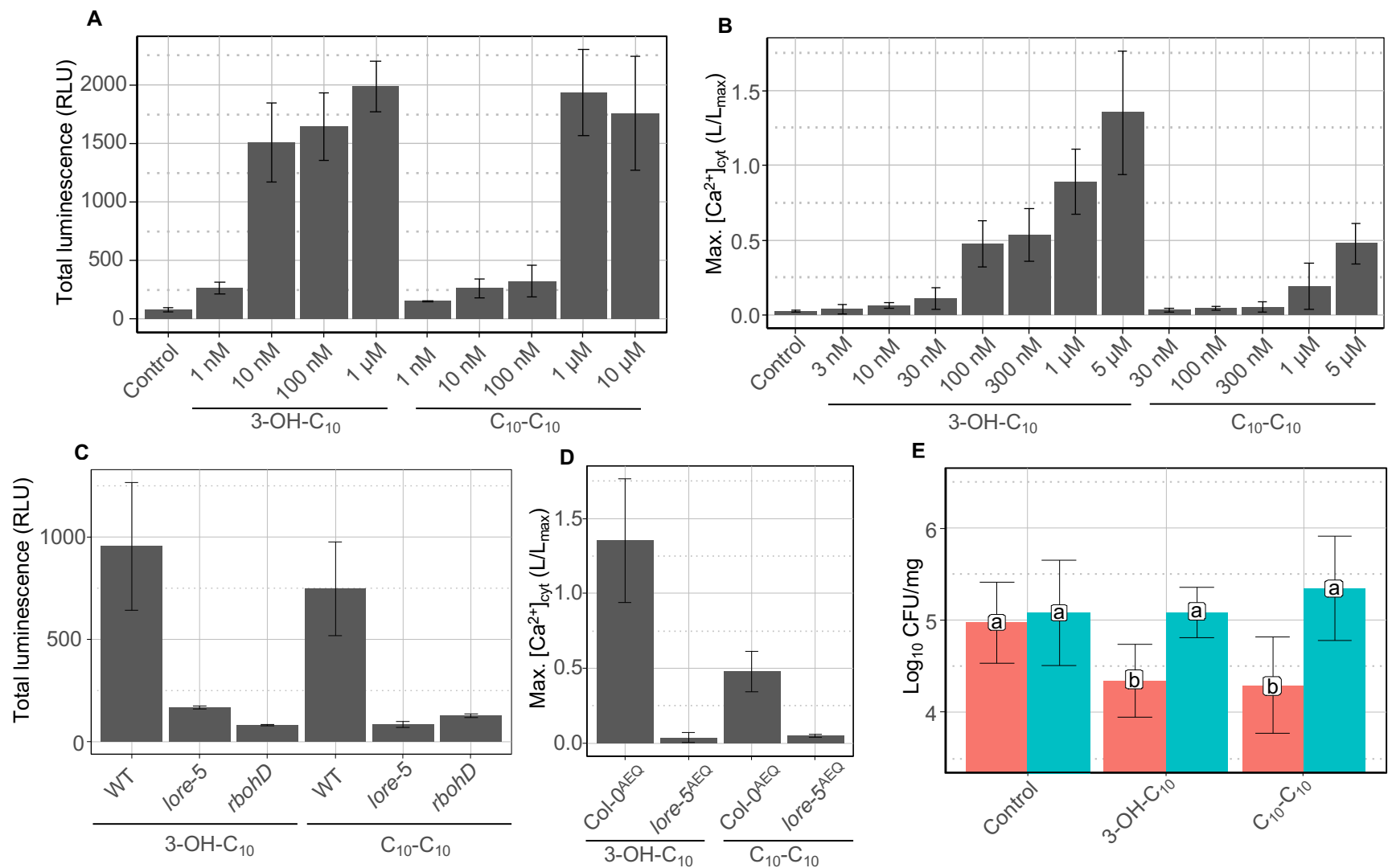


Fig. 3. Purified HAAs from *P. aeruginosa* trigger a LORE-dependent immune response in *Arabidopsis*. (A) Dose effect of 3-OH-C₁₀ and C₁₀-C₁₀ purified from *P. aeruginosa* on ROS production by WT leaf petioles. EtOH was used as negative control. Data are mean ± SEM (n = 6). Experiments have been realized twice with similar results. (B) Maximum (Max.) increases in [Ca²⁺]_{cyt} in *Arabidopsis* Col-0^{AEG} seedlings treated with different concentrations of 3-OH-C₁₀, C₁₀-C₁₀ purified from *P. aeruginosa* or MeOH as control. Data are mean ± SD (n = 3). Experiments have been realized twice with similar results. (C) ROS production measured after treatment of WT, *lore-5*, or *rbohD* leaf petioles with 10 μM 3-OH-C₁₀, 10 μM purified C₁₀-C₁₀ or EtOH as control. Data are mean ± SEM (n = 6). Experiments have been realized three times with similar results. (D) Maximum (Max.) increases in [Ca²⁺]_{cyt} in *Arabidopsis* Col-0^{AEG} and *lore-5*^{AEG} seedlings treated with 5 μM 3-OH-C₁₀ or purified C₁₀-C₁₀. Data are mean ± SD (n = 3). Experiments have been realized twice with similar results. For B and D, the same Col-0^{AEG} 5μM data are presented (same experiments). (E) WT (red) and *lore-5* (blue) *Arabidopsis* leaves were treated with 10 μM 3-OH-C₁₀, 10 μM purified C₁₀-C₁₀ or EtOH (control) 48 h before infection. *Pst* titers were measured at 3 d.p.i. Data are mean ± SD (n = 27, 31, 38, 13, 30, 37 (left to right)). Experiments have been realized twice with similar results. Letters represent data of pairwise Wilcoxon-Mann-Whitney statistic test with *P* > 0.05 (same letters) or *P* ≤ 0.05 (different letters).

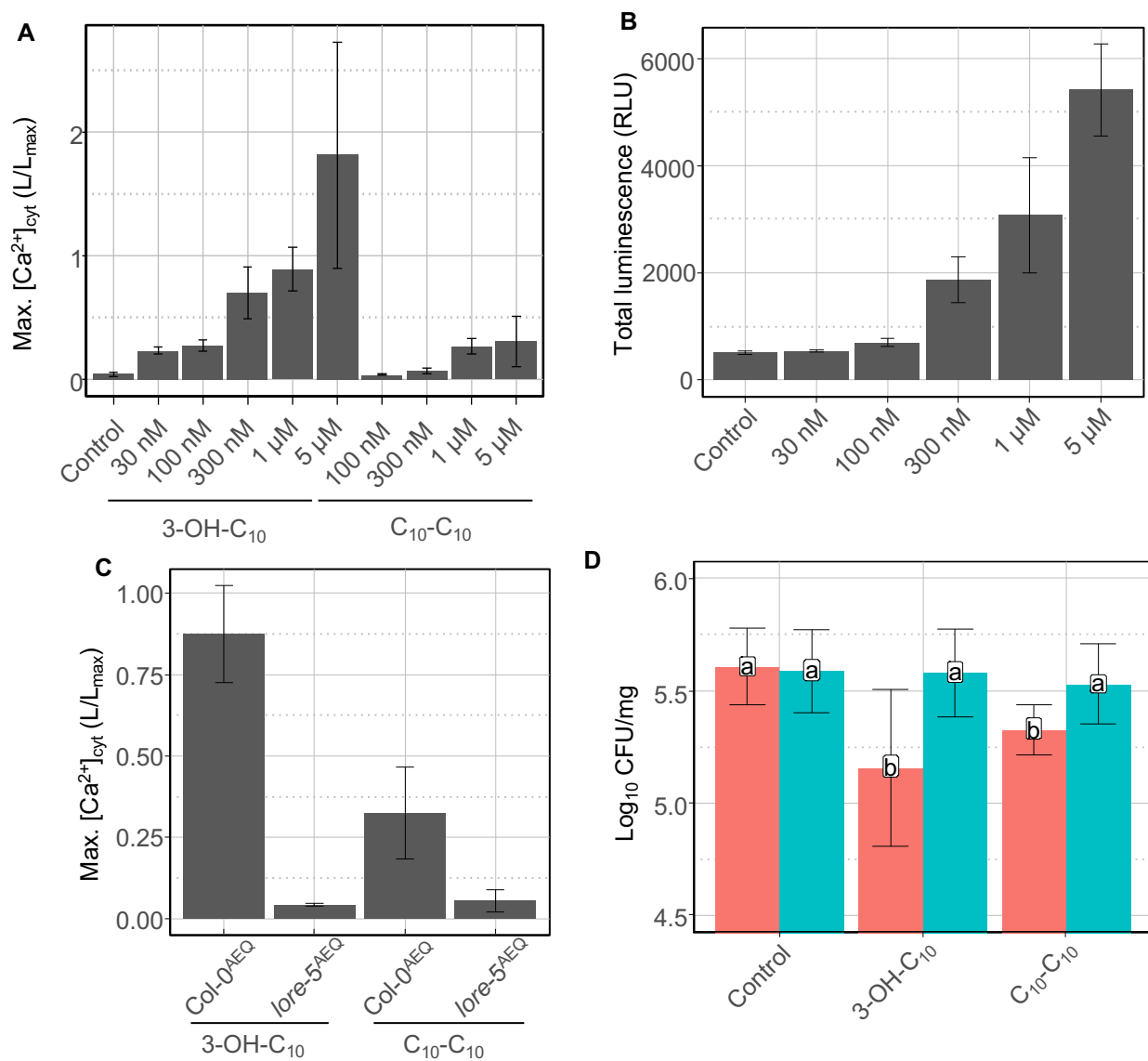


Fig. 4. Synthetic HAAs trigger a LORE-dependent immune response in *Arabidopsis*. (A) Maximum (Max.) increases in $[Ca^{2+}]_{cyt}$ in *Arabidopsis* Col-0^{AEQ} seedlings treated with different concentrations of 3-OH-C₁₀, synthetic C₁₀-C₁₀ or MeOH. Data are mean \pm SD (n = 3). Experiments have been realized twice with similar results. (B) Dose effect of synthetic C₁₀-C₁₀ on ROS production by WT leaf petioles. EtOH was used as negative control. Data are mean \pm SEM (n = 6). Experiments have been realized twice with similar results. (C) Maximum (Max.) increases in $[Ca^{2+}]_{cyt}$ in *Arabidopsis* Col-0^{AEQ} and lore-5^{AEQ} seedlings treated with 5 μ M 3-OH-C₁₀, synthetic C₁₀-C₁₀ or MeOH. Data are mean \pm SD (n = 3). Experiments have been realized twice with similar results. (D) WT (red) and lore-5 (blue) *Arabidopsis* leaves were treated with 10 μ M 3-OH-C₁₀, 10 μ M synthetic C₁₀-C₁₀, or MeOH (control) 48 h before infection. *Pst* titers were measured at 3 d.p.i. Data are mean \pm SD (n = 17, 21, 21, 30, 14, 30 (left to right)). Experiments have been realized twice with similar results. Letters represent data of pairwise Wilcoxon-Mann-Whitney statistic test with $P > 0.05$ (same letters) or $P \leq 0.05$ (different letters).

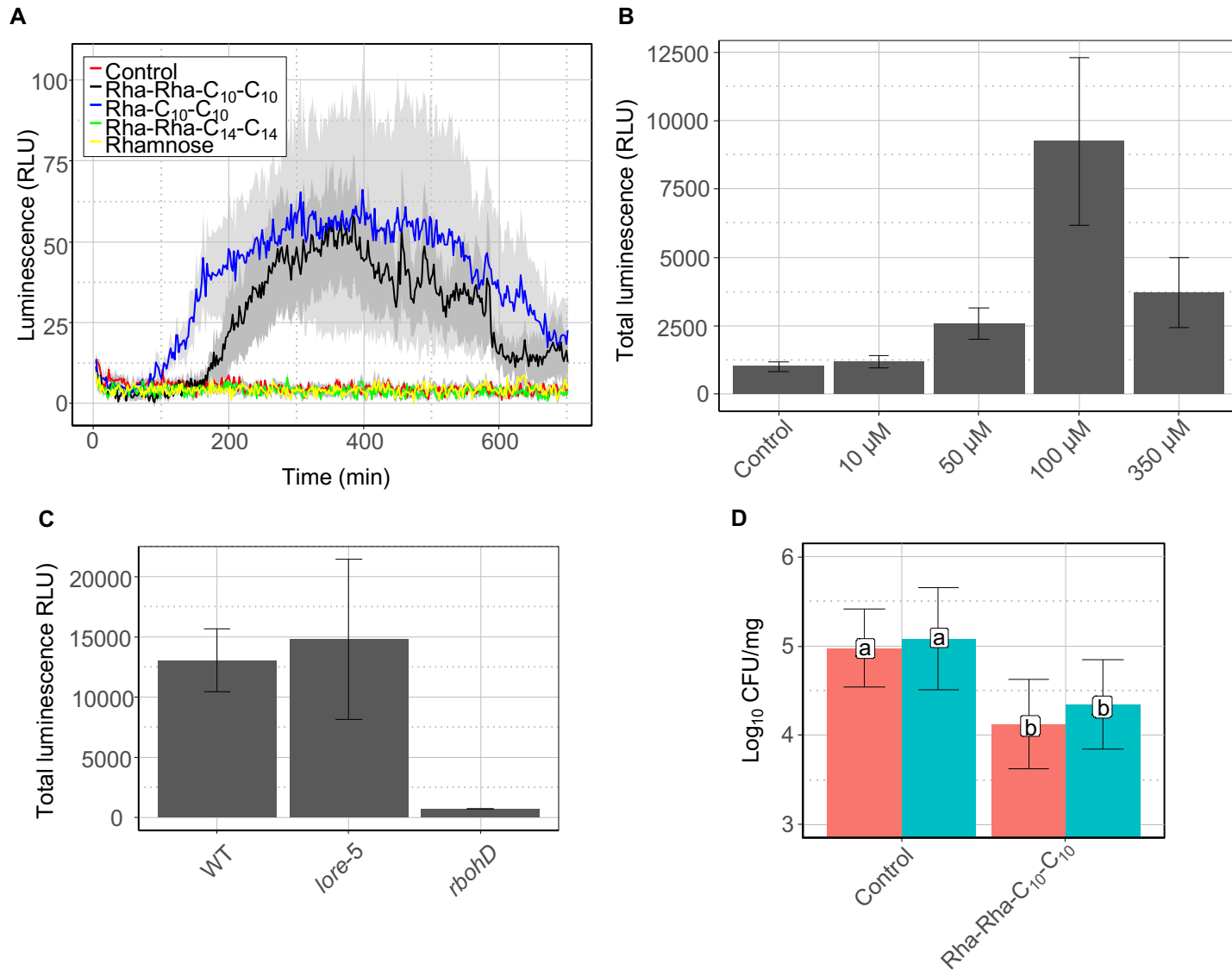


Fig. 5. Purified RLs trigger a LORE-independent *Arabidopsis* immune response. (A) Extracellular ROS production after treatment of WT leaf petioles with 100 μ M RLs, 100 μ M L-rhamnose, or EtOH (control). Data are mean \pm SEM (n = 6). (B) Dose effect of Rha-Rha-C₁₀-C₁₀ on ROS production. ROS production measured after treatment of WT leaf petioles with the indicated concentrations of Rha-Rha-C₁₀-C₁₀ or EtOH (control). Data are mean \pm SEM (n = 6). (C) ROS production measured after treatment of WT, *lore-5*, or *rbohD* leaf petioles with 100 μ M Rha-Rha-C₁₀-C₁₀. Data are mean \pm SEM (n = 6). (D) WT (red) and *lore-5* (blue) *Arabidopsis* leaves were treated with 10 μ M Rha-Rha-C₁₀-C₁₀ or EtOH (control) 48 h before infection. *Pst* titers were measured at 3 d.p.i. Data are mean \pm SD (n = 27, 31, 30, 26 (left to right)). Letters represent data of pairwise Wilcoxon-Mann-Whitney statistic test with $P > 0.05$ (same letters) or $P \leq 0.05$ (different letters). (A-D) Experiments have been realized three times with similar results.

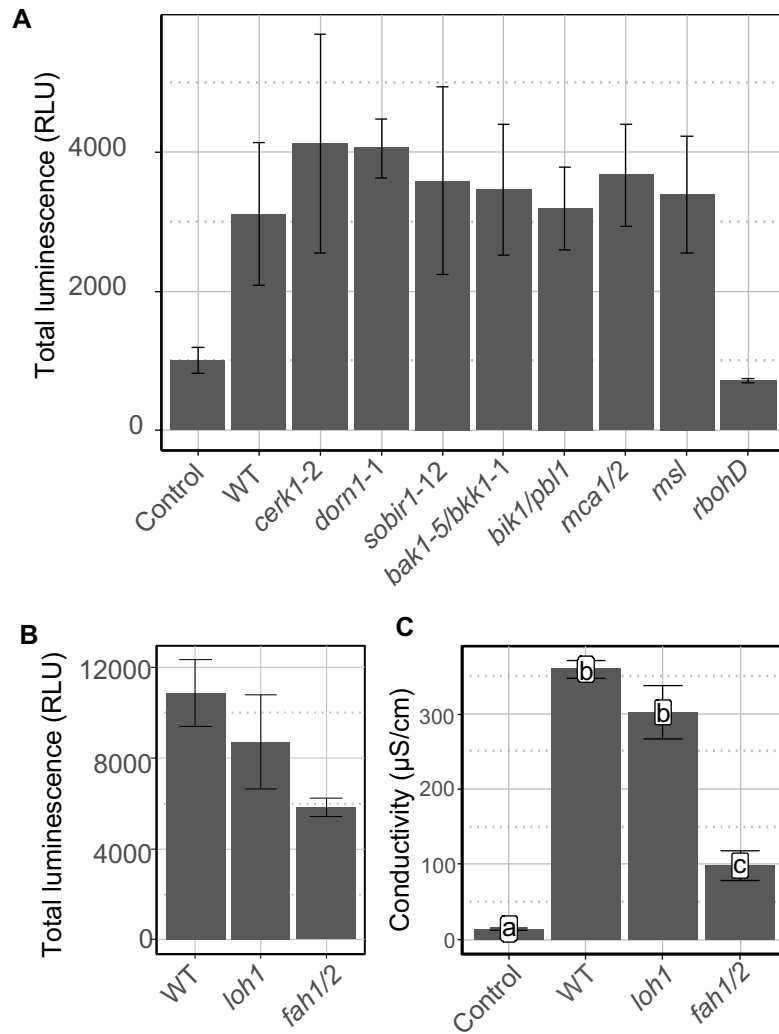
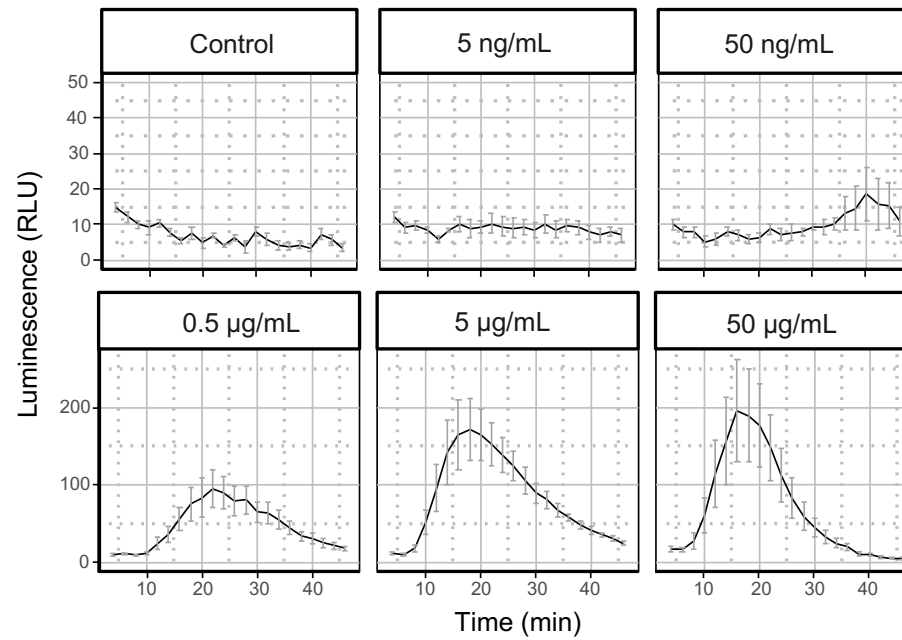
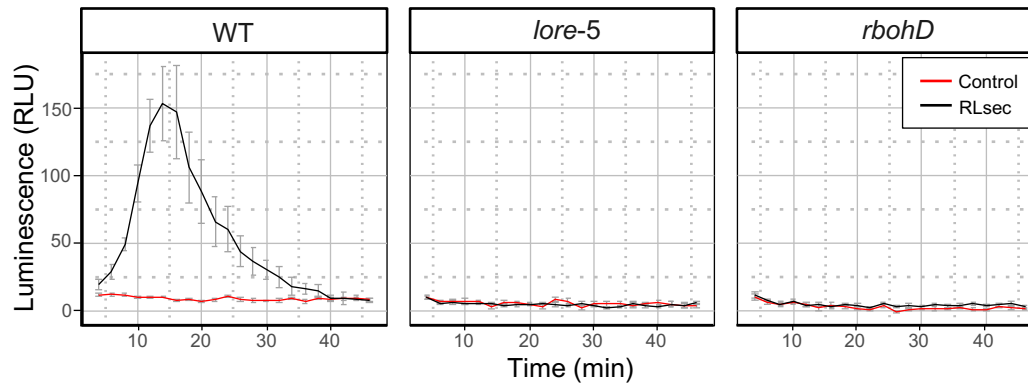


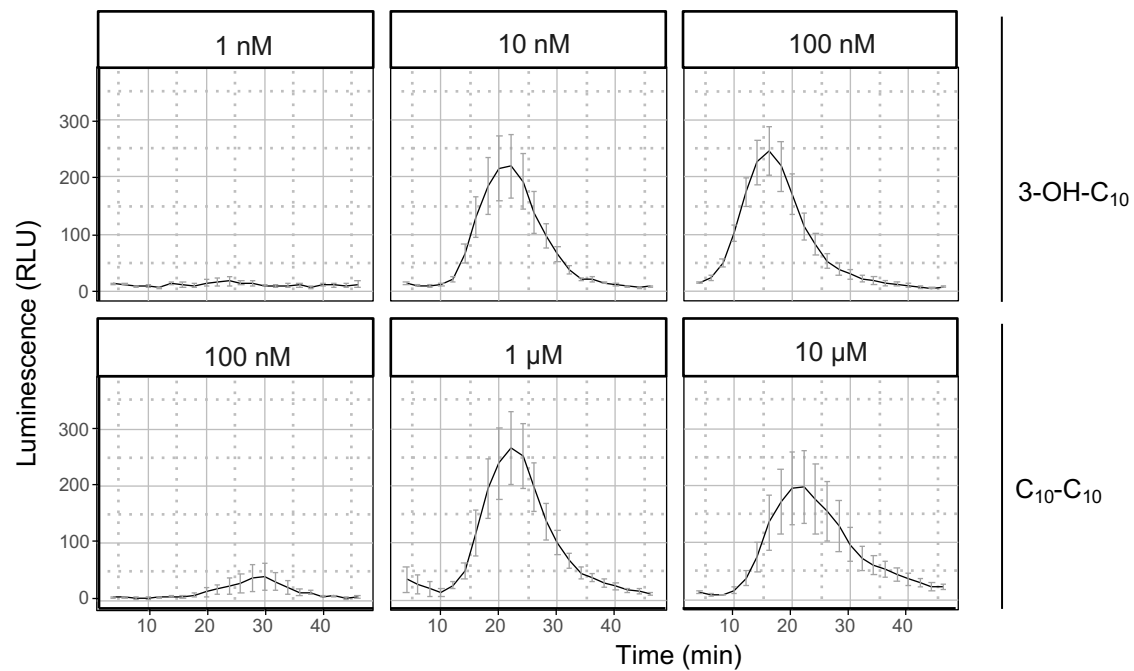
Fig. 6. RL perception is impacted by plasma membrane sphingolipid composition. Extracellular ROS production after treatment of (A) WT, *cerk1-2*, *dorn1-1*, *sobir1-12*, *bak1-5/bkk1-1*, *bik1/pbl1*, *mca1/2*, *msl4/5/6/9/10* (*msl*), or *rbohD*, and (B) WT, *loh1*, or *fah1/2* *Arabidopsis* leaf petioles with 100 μ M Rha-Rha-C₁₀-C₁₀ or EtOH (control). Data are mean \pm SEM (n = 6). Experiments have been realized three times with similar results. (C) Electrolyte leakage induced by 100 μ M Rha-Rha-C₁₀-C₁₀ or EtOH (Control) on WT, *loh1*, or *fah1/2* *Arabidopsis* leaf discs 24h post treatment. Data are mean \pm SEM (n = 6). Letters represent data of pairwise Wilcoxon-Mann-Whitney statistic test with $P > 0.05$ (same letters) or $P \leq 0.05$ (different letters). Experiments have been realized twice with similar results.



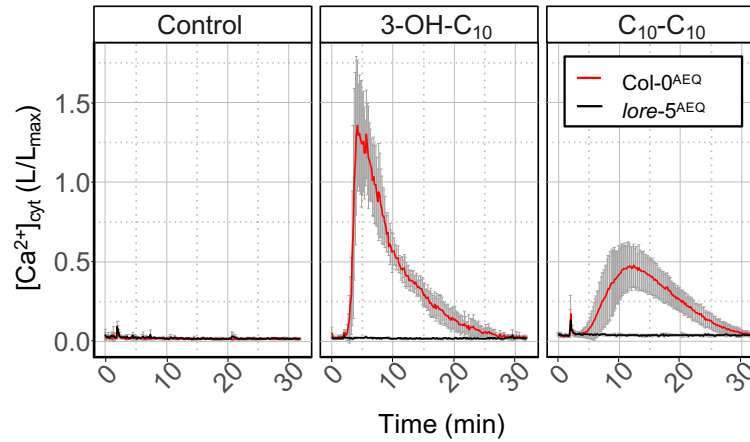
Supplementary fig. 1. RLsec dose effect on ROS. ROS production measured after treatment of WT leaf petioles with RLsec at the indicated concentrations or EtOH (control). Data are mean \pm SEM (n = 6). Experiments have been realized three times with similar results. The data presented here as kinetic are from the same experiments illustrated in fig. 1B.



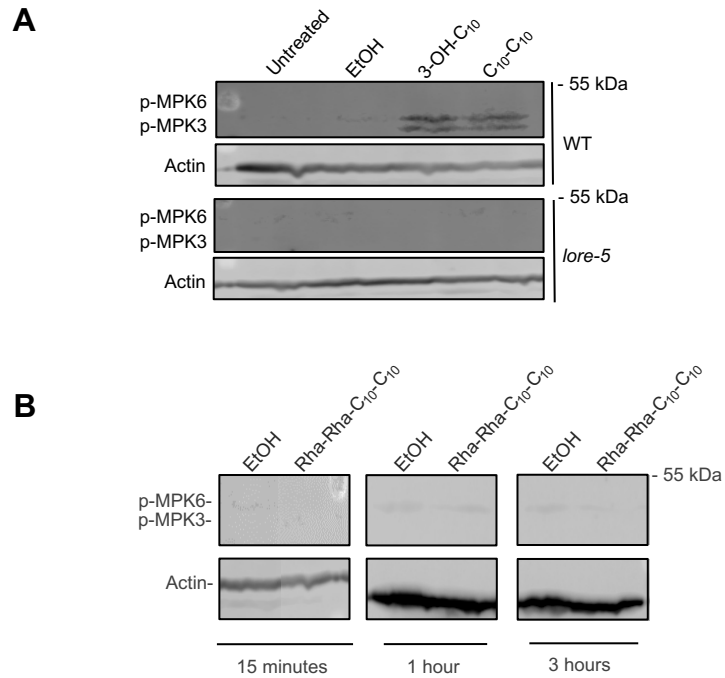
Supplementary fig. 2. RLsec induce early ROS production through LORE and RBOHD in *Arabidopsis*. Extracellular ROS production after treatment of WT, *lore-5*, or *rbohD* leaf petioles with 50 $\mu\text{g}/\text{mL}$ RLsec or EtOH (control). Data are mean \pm SEM (n = 6). Experiments have been realized three times with similar results. The data presented here as kinetic are from the same experiments illustrated in fig. 1C.



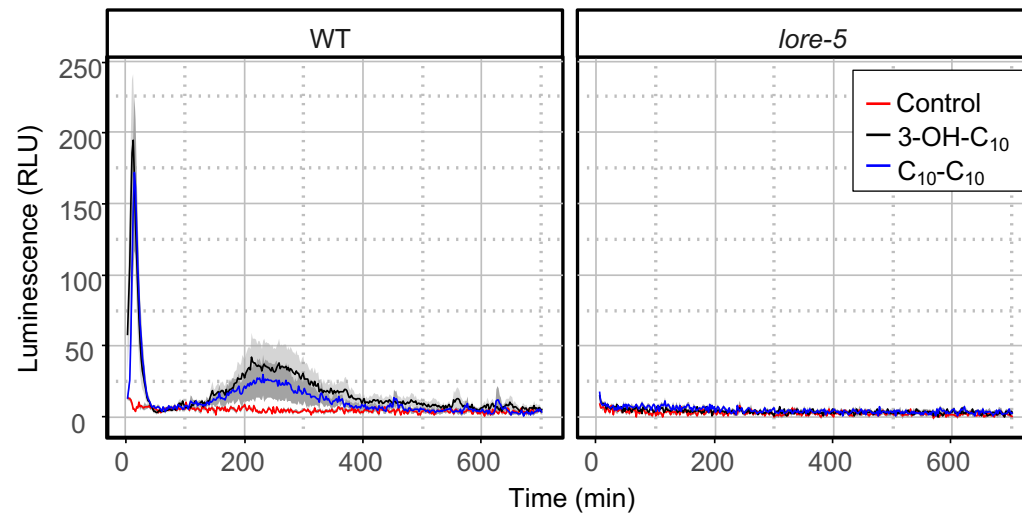
Supplementary fig. 3. Dose effect of 3-OH-C₁₀ and C₁₀-C₁₀ purified from *P. aeruginosa* on ROS production. ROS production measured after treatment of WT leaf petioles with the indicated concentrations of 3-OH-C₁₀ and purified C₁₀-C₁₀. Data are mean ± SEM (n = 6). Experiments have been realized twice with similar results. The data presented here as kinetic are from the same experiments illustrated in fig. 3A.



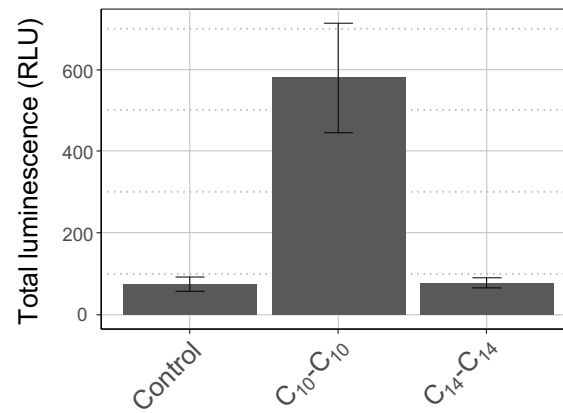
Supplementary fig. 4. Time course Ca²⁺ signaling. [Ca²⁺]_{cyt} over time in Col-0^{AEQ} and *lore-5*^{AEQ} seedlings after treatment with 5 μM purified C₁₀-C₁₀, 5 μM 3-OH-C₁₀ or MeOH (control). Data are mean ± SD (n = 3). Experiments have been realized twice with similar results. The data presented here as kinetic are from the same experiments illustrated in fig. 3B.



Supplementary fig. 5. MAPK assay. Activation of MPK3 and MPK6 in (A) WT and *lore-5* leaf disk 15 minutes after treatment with 10 μ M 3-OH-C₁₀, 10 μ M purified C₁₀-C₁₀ or EtOH; (B) WT leaf disk 15 minutes, 1 hour, and 3 hours after treatment with 100 μ M Rha-Rha-C₁₀-C₁₀ or EtOH. Actin was used as loading control. Experiments have been realized twice with similar results.



Supplementary fig. 6. ROS production measured after treatment of WT or *lore-5* leaf petioles with 10 μ M 3-OH-C₁₀, 10 μ M purified C₁₀-C₁₀ or EtOH (control). Data are mean \pm SEM (n = 6). Experiments have been realized twice with similar results.



Supplementary fig. 7. Chain length of HAAs impact *Arabidopsis* ROS immune response. ROS production measured after treatment of WT leaf petioles with 10 μ M of purified C₁₀-C₁₀ from *Pseudomonas aeruginosa*, C₁₄-C₁₄ purified from *Burkholderia glumae* or with EtOH (control). Data are mean \pm SEM (n = 6). Experiments have been realized three times with similar results.

Molecule	% (dry weight)
3-OH-C₈, 3-OH-C₁₀, 3-OH-C₁₂	0.37
HAAs	3.75
C ₈ -C ₈	0.23
C ₈ -C ₁₀	0.85
C ₁₀ -C ₁₀	2.13
C ₁₀ -C ₁₂	0.26
C ₁₂ -C ₁₂	0
C ₈ -C _{12:1}	0.09
C ₁₀ -C _{12:1}	0.12
C ₁₂ -C _{12:1}	0.07
monorhamnolipids	50.94
Rha-C ₈ -C ₈	0
Rha-C ₈ -C ₁₀	5.28
Rha-C ₁₀ -C ₁₀	37.61
Rha-C ₁₀ -C ₁₂	3.53
Rha-C ₁₂ -C ₁₂	0.06
Rha-C ₈ -C _{12:1}	0.72
Rha-C ₁₀ -C _{12:1}	3.55
Rha-C ₁₂ -C _{12:1}	0.19
dirhamnolipids	44.94
Rha-Rha-C ₈ -C ₈	0.36
Rha-Rha-C ₈ -C ₁₀	4.33
Rha-Rha-C ₁₀ -C ₁₀	33.14
Rha-Rha-C ₁₀ -C ₁₂	4.22
Rha-Rha-C ₁₂ -C ₁₂	0.10
Rha-Rha-C ₈ -C _{12:1}	0.64
Rha-Rha-C ₁₀ -C _{12:1}	1.88
Rha-Rha-C ₁₂ -C _{12:1}	0.27

Supplementary table 1. RLsec composition. Distribution of congeners (percent) present in the lipidic secretome produced by *P. aeruginosa* (Jeneil, JBR-599, lot. #050629).

Molecules	Origin	Reference	Sample concentration (for quantification)	Free 3-OH-C ₁₀ concentration	Sample concentrations (for biological assays)	Concentration of 3-OH-C ₁₀ at the compound concentration used for the experiments	MTI in <i>Arabidopsis</i>	LORE-dependent
Mono-RL (Rha-C₁₀-C₁₀)	<i>Pseudomonas aeruginosa</i> PA14	36	5 mM	0.28 μM	100 μM	5 nM	Yes	No
Di-RL (Rha-Rha-C₁₀-C₁₀)	<i>Pseudomonas aeruginosa</i> PA14	36	5 mM	0.05 μM	10 μM to 350 μM	100 pM to 3 nM	Yes	No
Di-RL (Rha-Rha-C₁₄-C₁₄)	<i>Burkholderia glumae</i>	53	nd	nd	100 μM	nd	No	No
C₁₄-C₁₄	<i>Burkholderia glumae</i>	this study	1 mM	<LOQ	10 μM	<LOQ	No	No
C₁₀-C₁₀	<i>Pseudomonas aeruginosa</i> PA14	this study	0.1 mM	0.09 μM	1 nM to 10 μM	0.9 pM to 9 nM	Yes	Yes
Synthetic C₁₀-C₁₀	Chemical synthesis (see Supplementary data 1 and 2)	this study	0.1 mM	<LOQ	30 nM to 10 μM	<LOQ	Yes	Yes

Supplementary table 2. Quantification of free 3-OH-C₁₀ in HAA and RL samples.